Electron-optical phase shift of a Josephson vortex

Marco Beleggia
Materials Science Department, Brookhaven National Laboratory, Upton, New York 11973, USA
(Received 9 September 2003; published 30 January 2004)

The possibility of directly observing Josephson vortices in a superconducting material by transmission electron microscopy is here investigated. First, the anisotropic London equation for the magnetic field of a Josephson vortex is solved in Fourier space. Then, from the knowledge of the magnetic field, the vector potential and the Aharonov-Bohm phase shift are derived. Finally, phase contrast image simulations are presented. It will be shown that, with current technology, the direct observation of a Josephson vortex is possible.

DOI: 10.1103/PhysRevB.69.014518 PACS number(s): 74.78.Bz, 68.37.Lp, 61.14.Nm

I. INTRODUCTION

Recent transmission electron microscopy (TEM) experiments performed on high-T_c superconductors[1–3] clearly shows the formation of one-dimensional vortex chains in $YBaCu_3O_{7-\delta}$ (YBCO) and $Bi_2Sr_2CaCu_2O_{8+\delta}$ (BSSCO). The mechanism of formation of these chains is currently under intensive investigation. It was proposed in Ref. 3 that the formation of the chains in BSSCO may be related to the presence of a Josephson vortex (JV) which aligns the standard (Abrikosov or pancake) vortices along its core. A possible mechanism of interaction between pancake vortices in a layered superconductor and the JV which may lead to the formation of chains was suggested in Ref. 4. A theoretical investigation, which will be followed by experimental research, is now in progress in order to ascertain if the presence of the JV can be inferred indirectly from the expected effects of this interaction. However, it would be more fruitful to observe directly a JV in TEM, and to verify the correlation between the regular vortex lattice and the JV (or the JV lattice). Unfortunately, the only attempt mentioned in the literature[3] to directly observe the JV underneath the chain failed, due to unfavorable experimental conditions. It is the main purpose of this paper to show that an experimental setup that may allow for direct observation of a JV can be found.

An extensive literature is available for the description of a JV.[5,6] However, the analysis up to now does not include the calculation of the vector potential and corresponding phase shift. The aim of the first part of this paper is to extend the available description of a JV in a thin film, including the change in magnetic-field topography induced by the presence of the specimen surfaces and the vector potential. Then, following the Fourier space approach recently introduced as a theoretical scheme for the investigation of superconducting vortices by TEM,[7–9] the electron-optical phase shift associated with the JV will be calculated analytically. Finally, after extracting all the possible information from the phase shift, image simulations will be shown in order to sustain the proposed experimental setup and the feasibility of the experiments.

II. MAGNETIC FIELD

The magnetic field **B** of a JV oriented along the x axis of a Cartesian reference system (see Fig. 1) satisfies the anisotropic London equation

$$\mathbf{B}-\boldsymbol{\nabla}\times(\Lambda\cdot\boldsymbol{\nabla}\times\mathbf{B})=\phi_0\,\delta(y)\,\delta(z)\hat{\mathbf{x}}. \tag{1}$$

Here Λ is the anisotropy tensor for a uniaxial material,

$$\Lambda=\begin{pmatrix}\lambda^2 & 0 & 0\\ 0 & \lambda^2 & 0\\ 0 & 0 & \lambda_c^2\end{pmatrix}, \tag{2}$$

where λ and λ_c are the penetration depths in the ab plane and along the c axis, respectively (their ratio $\gamma=\lambda_c/\lambda$ is the anisotropy factor of the material). The London equation is particularly suitable for the description of a JV. In fact, the right-hand side of Eq. (1) describes a core of vanishing extension, which is what a JV is expected to have.[5]

As the vortex lies along the x axis, the only nonvanishing component of the field is B_x, which is a function of y and z only, because the vortex is of infinite extension, which means invariance along x. We can therefore write the London equation (1) for B_x explicitly, considering that the ∂_x component of the $\boldsymbol{\nabla}$ operator is zero and that the other two components of the field are trivially zero:

$$B_x-(\lambda_c^2\partial_y^2+\lambda^2\partial_z^2)B_x=\phi_0\,\delta(y)\,\delta(z). \tag{3}$$

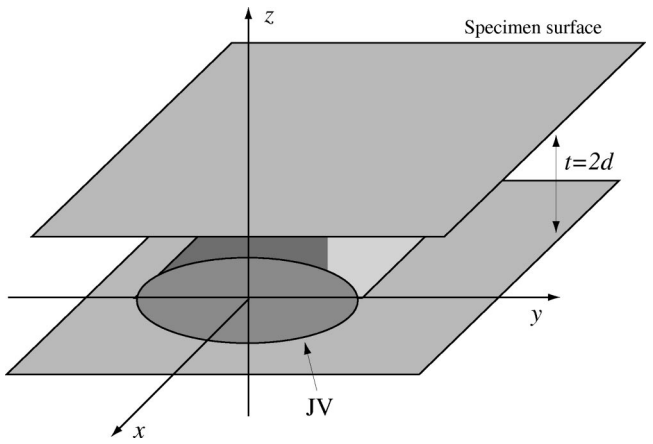

FIG. 1. Schematic view of a Josephson vortex in a superconducting thin film of thickness $t=2d$.

Before analyzing the effect of the specimen surfaces, it is necessary to determine the bulk solution B_x^b. In a (k_y,k_z) 2D Fourier space, where each partial derivative ∂_j is transformed in ik_j, Eq. (3) reads

$$\tilde{B}_x+(\lambda_c^2k_y^2+\lambda^2k_z^2)\tilde{B}_x=\phi_0, \tag{4}$$

whose solution is

$$\tilde{B}_x^b=\frac{\phi_0}{1+\lambda_c^2k_y^2+\lambda^2k_z^2}, \tag{5}$$

which, formally, can be inverse transformed to real space as

$$B_x^b=\frac{\phi_0}{4\pi^2}\int\int\frac{dk_ydk_z}{1+\lambda_c^2k_y^2+\lambda^2k_z^2}e^{iyk_y}e^{izk_z}. \tag{6}$$

We can easily perform the integration over k_z, and consider the symmetry of the field along y, obtaining

$$B_x^b(y,z)=\frac{\phi_0}{2\pi\lambda}\int_0^\infty\frac{\cos(yk_y)}{Q}e^{-(|z|/\lambda)Q}dk_y, \tag{7}$$

with $Q=\sqrt{1+\lambda_c^2k_y^2}$.

The real-space expression of B_x can be found by integrating with respect to k_y, and the result is, as expected,

$$B_x^b(y,z)=\frac{\phi_0}{2\pi\lambda\lambda_c}K_0\left(\sqrt{\frac{y^2}{\lambda_c^2}+\frac{z^2}{\lambda^2}}\right). \tag{8}$$

To introduce the effect of the specimen surfaces, located at $z=\pm d$ (see again Fig. 1), we go back to the London equation, searching for a more general solution. As Eq. (3) is an inhomogeneous second-order partial differential equation, and we have already obtained a particular solution B_x^b, to accommodate the presence of an interface at the specimen surface we only need to find the general solution of the homogeneous equation and impose the correct boundary conditions.

The general solution of the homogeneous London equation can be conveniently expressed as

$$B_x^s(y,z)=\frac{\phi_0}{2\pi\lambda}\int_0^\infty\frac{\cos(yk_y)}{Q}H(k_y)\cosh\left(\frac{z}{\lambda}Q\right)dk_y, \tag{9}$$

where the unknown function $H(k_y)$ is to be determined by the application of the boundary conditions at the specimen surface. We chose the hyperbolic cosine, rather than the more generic sum of exponentials, because we have already exploited the symmetry of the field. In this way, we may apply the boundary condition at the upper surface $z=d$ only.

As the field is identically zero in the vacuum, the boundary condition is simply $B_x(y,d)=0$, which means

$$e^{-(|z|/\lambda)Q}+H(k_y)\cosh\left(\frac{d}{\lambda}Q\right)=0, \tag{10}$$

which gives the solution for $H(k_y)$. The total magnetic field, which takes into account the effect of the specimen surfaces, is therefore

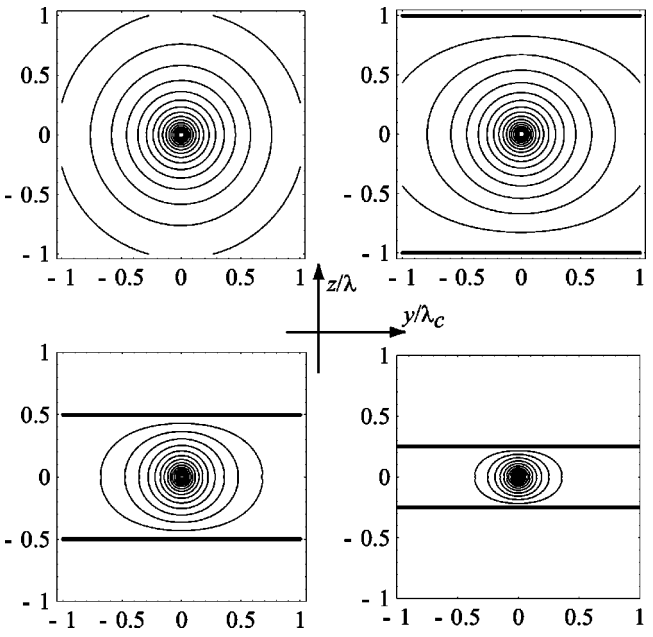

FIG. 2. Contour plot of the magnetic field associated with a Josephson vortex. (a) JV in a bulk material ($t=\infty$); (b) field in a specimen of thickness $t=2\lambda$; (c) $t=\lambda$; (d) $t=\lambda/2$. Each field contour line represents a step of $\phi_0/(10\pi\gamma\lambda^2)$ (e.g., 3.3 G for $\lambda=200$ nm and $\gamma=5$).

$$B_x(y,z)=\frac{\phi_0}{2\pi\lambda}\int_0^\infty dk_y\frac{\cos(yk_y)}{Q}\left[\cosh\left(\frac{z}{\lambda}Q\right)\tanh\left(\frac{d}{\lambda}Q\right)-\sinh\left(\frac{|z|}{\lambda}Q\right)\right]. \tag{11}$$

A contour plot of the x component of the magnetic field is reported in Fig. 2. It can be seen that decreasing the specimen thickness from $t=\infty$ (bulk reference case) (a) to $t=\lambda/2$ (d), the JV appears to decrease in size. In Fig. 2, as the y and z directions are plotted on a different length scale (y/λ_c and z/λ), the real dimensions are actually stretched by a factor γ along y.

III. VECTOR POTENTIAL AND PHASE SHIFT

As the magnetic field has only one component, we can safely assume that the vector potential has the form $(0,0,A_z)$ in such a way that $\mathbf{B}=\nabla\times\mathbf{A}=(\partial_yA_z,0,0)$, or $B_x=\partial_yA_z$. It can be verified that the following vector potential

$$A_z(y,z)=\frac{\phi_0}{2\pi\lambda}\int_0^\infty dk_y\frac{\sin(yk_y)}{k_yQ}\left[\cosh\left(\frac{z}{\lambda}Q\right)\tanh\left(\frac{d}{\lambda}Q\right)-\sinh\left(\frac{|z|}{\lambda}Q\right)\right] \tag{12}$$

correctly generates the previously found magnetic field. Moreover, it satisfies $\nabla\cdot\mathbf{A}=0$, and it vanishes at infinity.

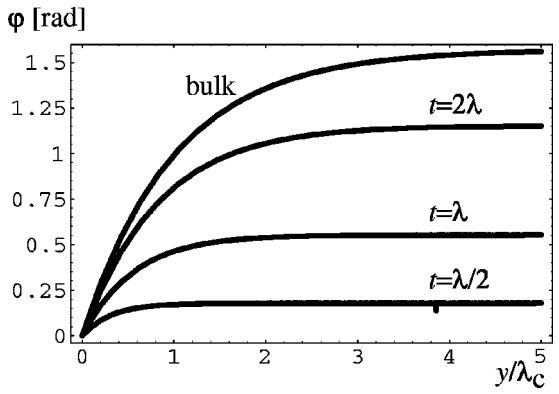

FIG. 3. Phase shift of a Josephson vortex for different values of the specimen thickness as a function of the distance from the core. For negative y values, the phase shift has odd symmetry.

The magnetic phase shift can be calculated from the standard Aharonov-Bohm expression (see, e.g., Refs. 10 and 11), adapted to our case,

$$\varphi(y)=\frac{\pi}{\phi_0}\int_{-d}^{+d}A_z(y,z)dz. \tag{13}$$

The line integral is performed only within the specimen, because above and below the surfaces, both the magnetic field and the vector potential are identically zero if the specimen is considered of infinite extension in the (x,y) plane. The finite extension of the specimen, namely, a specimen edge where the JV terminates, would give a small negative contribution to the phase shift due to the field lines which have to form a closed loop. Since this contribution is inversely proportional to the JV length (more precisely to the JV length/width ratio), it is neglected because we assume that the specimen edge is sufficiently far away from the region of observation.

The result for the phase shift, after the integration along z, turns out to be

$$\varphi(y)=\int_0^\infty dk_y\frac{\sin(yk_y)}{k_yQ^2}\left[1-\mathrm{sech}\left(\frac{d}{\lambda}Q\right)\right], \tag{14}$$

whose plot is reported in Fig. 3 for different anisotropy factors and specimen thicknesses.

It is worthwhile noting that the total phase shift $\varphi_t=\varphi(\infty)-\varphi(-\infty)=2\varphi(\infty)$ is not identically equal to π as one may expect from the fact that the vortex is carrying a single flux quantum. Rather surprisingly, the total phase shift can be evaluated as

$$\varphi_t=2\lim_{y\to\infty}\varphi(y)=\pi\left[1-\mathrm{sech}\left(\frac{d}{\lambda}\right)\right], \tag{15}$$

which is equal to π only in the limit $d\gg\lambda$ (bulk case). The previous result was obtained considering that in the framework of distribution theory

$$\lim_{y\to\infty}\frac{\sin(yk_y)}{k_y}=\frac{\pi}{2}\delta(k_y). \tag{16}$$

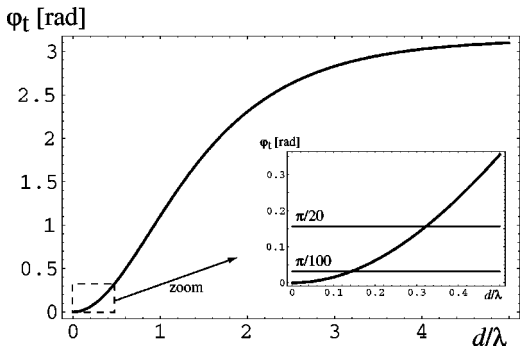

FIG. 4. Total phase shift φ_t as a function of the reduced specimen thickness d/λ. In the inset, the ultrathin region is displayed together with two reference phase values of $\pi/20$ and $\pi/100$.

The plot of the total phase shift is reported in Fig. 4. The decrease of the total phase shift in very thin films of isotropic superconducting material has been also noticed in Ref. 12.

Incidentally, we may note that the profile displayed in Fig. 4 is indicative of the phase shift associated with a Josephson vortex also when its axis does not follow the $\hat{\mathbf{x}}$ direction throughout the entire specimen, provided that the line scan is taken along the perpendicular to the local direction of the JV axis. In fact, the total phase shift is directly proportional to the magnetic flux carried by the JV, and the total flux is not dependent on the JV axis being along $\hat{\mathbf{x}}$ or following some regular curved path in the (x,y) plane. Therefore, if the JV follows curved paths, possibly because of material defects or disorder present in the sample, the total phase shift, Eq. (15), remains accurate.

It is important to emphasize that the total phase shift φ_t *does not* depend on anisotropy. The role of anisotropy is to change the spatial distribution of the phase shift along the y axis (as shown in Fig. 3). This apparently negligible detail leaves some hope to detect the Josephson vortex in a thin TEM sample. In fact, there are two major constraints imposed on the experiments: first, the total phase shift must be larger than the limit of the phase retrieval technique employed; and second, the phase shift must be localized inside the field of view of the recorded image. Only the second requirement, as it will be now demonstrated, is strongly affected by anisotropy.

We can provide an estimate of the spatial extent of the phase shift, introducing the *vortex width*, whose geometrical definition is explained in the inset of Fig. 5. The width w can be calculated from the phase derivative in the origin and from the total phase shift

$$w=\frac{\varphi_t}{\varphi'(0)}=\xi\lambda_c, \tag{17}$$

where the factor ξ can be evaluated numerically from

$$\frac{1}{\xi}=\frac{1}{\varphi_t}\int_1^\infty\frac{dq}{q}\frac{1-\mathrm{sech}(qd/\lambda)}{\sqrt{q^2-1}}. \tag{18}$$

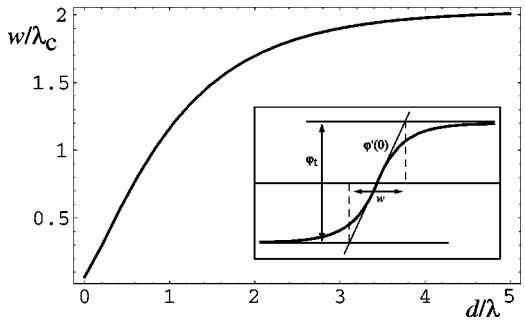

FIG. 5. Apparent width of a Josephson vortex, measured in λ_c units, plotted as a function of the reduced specimen thickness d/λ.

While the factor ξ is a nontrivial function of the ratio d/λ, the vortex diameter turns out to be linear in λ_c. The plot of w/λ_c as a function of d/λ is reported in Fig. 5. As a remark, it is necessary to point out that the parameter w is only an estimate of the spatial extent of the phase shift, and should not be extrapolated outside of the geometrical definition here assumed. In particular, it cannot be directly correlated to the physical extent of the supercurrents, as the phase shift is a projected quantity. However, as the TEM images mainly depend on the phase shift, the evaluation of the phase extent is relevant.

For a thick specimen, when $d \gg \lambda$, the factor ξ converges to the value 2. This is consistent with the expectation for a bulk material, where the phase shift is purely exponential with a decay length equal to λ_c. For other ratios d/λ, the vortex width is affected by the specimen surfaces, and it appears to be more *concentrated*. In fact, as shown in Fig. 5, w goes to zero for very thin specimens. A non trivial mathematical analysis is necessary to evaluate the series expansion of the vortex width for very thin specimens. The final result is expressed in the following relation:

$$w = 1.35\gamma d, \tag{19}$$

valid only for $d \ll \lambda$. For a generic material with anisotropy factor $\gamma = 10$, the vortex width decreases from $w = 20\lambda$ in the bulk to $w = 2.7\lambda$ in a specimen of half thickness $d = \lambda/5$, which is roughly a factor of 8.

This result is rather surprising. Whenever surfaces are involved, consistently with what has always been observed, we would expect an enlargement of the vortex size with a decreasing thickness. For instance, in the case of Pearl vortices,[13] the spatial extent is related to λ^2/d, which diverges for $d \ll \lambda$. However, the situation here described cannot be compared easily with the results obtained when the vortex is perpendicular to the specimen surfaces. Here the vortex is parallel to the surfaces, and the surrounding vacuum plays a different role with respect to the perpendicular case.

Combining the two positive results of (i) a total phase shift only dependent on the ab penetration depth λ and (ii) a flux concentration for thin specimens, we can now clearly show that the direct observation of a Josephson vortex by TEM is feasible.

IV. JOSEPHSON VORTICES IN TEM

In order to give an explicit example of how a Josephson vortex should appear in the TEM, we will now consider the real cases of YBCO and BSSCO. The first is characterized by an ab penetration depth of the order of 200 nm and an anisotropy factor around 5, which means $\lambda_c = 1$ μm. The latter has instead a penetration depth around 300 nm and a very large anisotropy factor which can be taken equal to 200. The λ_c of BSSCO is therefore of the order of 60 μm.

To maximize the total phase shift, the specimen should be thick enough to ensure that the phase shift is larger than the sensitivity of the technique employed. In general, a conservative estimate of the minimum detectable phase shift can be taken to be $\pi/20$. Therefore, as $\varphi_t > \pi/20$ for $d/\lambda > 0.65$ [from Eq. (15)] the specimen thickness should be $t > 1.3\lambda$ or $t > 260$ nm in the case of YBCO. To be even more conservative, we may safely assume that $d = \lambda$ or $t = 400$ nm, which is well within the specifications of the 1 MV state-of-the art microscope developed in Japan.[14]

In terms of spatial extent of the phase shift, the main limitation is the field of view that can be recorded in a single image. Moreover, holography requires a large spatial coherence, in order to establish the interference pattern on the image. Finally, from a specimen preparation standpoint, it may be very difficult to prepare clean, flat single crystals of several microns in size. Therefore, it would be recommendable to keep the specimen thickness rather low, in order to exploit the surface-induced confinement effect of the josephson vortex. For $d = 0.65\lambda$, Eq. (18) gives the value $\xi = 0.8$, which means $w = 0.8$ μm. For the thicker specimen $d = \lambda$, the resulting width would be $w = 1.2$ μm in the YBCO case.

For BSSCO the situation is more delicate. To have a reasonable spatial extent, we have to decrease dramatically the specimen thickness, down to the limit of current phase retrieval techniques. Assuming that a phase shift as small as $\pi/50$ is detectable (it is stated in Ref. 15 that even $\pi/100$ can be achieved), we can decrease the specimen thickness down to $d = 0.2\lambda$, or $t = 120$ nm. This results in a phase spatial extent of 11 μm, which still is within the reach of the specimen preparation techniques and the electron-optical configuration of the microscope.

Phase and image simulations of Josephson vortices for the two cases of YBCO and BSSCO are shown in Figs. 6 and 7. In (a) the holographic contour map is displayed, properly amplified (16× for YBCO and 256× for BSSCO). The line scan of the phase shift across the vortex cross section is then shown in (b). In (c) the out-of-focus image simulation is shown, with a line scan displayed on the right in (d). The defocus distance, assuming an accelerating voltage of 1 MV, is 50 mm in the YBCO case and 10 m in the BSSCO case. The defocus value for the BSSCO is rather large, but the observation of vortices in superconductors by TEM often requires such distances due to the large size of the vortices. The contrast values obtained are above the usual limit of detectability (3%). The contrast obtained for YBCO (50%) is comparable, if not higher, to the standard contrast values in the observation of regular vortices. The image contrast is defined as $(I_{\max} - I_{\min})/(I_{\max} + I_{\min})$.

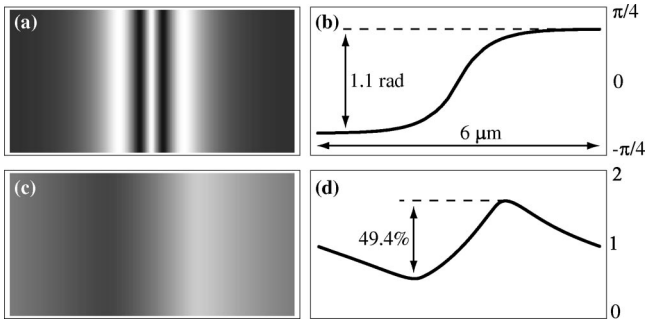

FIG. 6. Josephson vortex in YBCO: (a) holographic cosine map of the phase shift (16× amplified); (b) line scan of the phase shift across the vortex axis; (c) out-of-focus image (50 mm defocus) of the JV; (d) line scan of the out-of-focus image showing the 50% image contrast obtained.

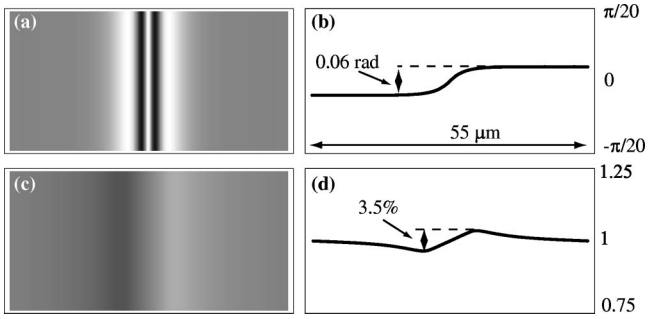

FIG. 7. Josephson vortex in BSSCO: (a) holographic cosine map of the phase shift (256× amplified); (b) line scan of the phase shift across the vortex axis; (c) out-of-focus image (10 m defocus) of the JV; (d) line scan of the out-of-focus image showing the 3.5% image contrast obtained.

V. CONCLUSIONS

The distances involved, and, in general, the requirements pointed out in this paper, are within the technical specification of modern microscopes. This strongly suggests that the direct observation of Josephson vortices by TEM is within reach, especially for low- or medium-anisotropy materials. For high-anisotropy material, such as BSSCO, the experiment appears to be challenging but possible. There is still room for improvement, especially considering that the phase retrieval techniques are endlessly progressing, both in accuracy and sensitivity. In a recent work[16] it is claimed that tiny phase shifts as small as $\pi/150$ would be detectable in TEM. This would allow a further reduction of the specimen thickness, which in turns would facilitate the specimen preparation. Finally, the electron microscope should be flexible enough to record Fresnel images at a very low magnification. This requires an electron-optical configuration which is not the standard for any microscope. However, defocus distances of several meters have been already reported[17] and in the observation of pancake vortices the vortex lattice is often imaged at a very low magnification. All considered, it can be clearly stated that there are no serious obstacles which may prevent the success of the proposed experiments. It is hope of the author that this theoretical investigation will stimulate the experimental research which may finally lead to the first direct observation by TEM of a Josephson vortex in a superconducting material.

ACKNOWLEDGMENTS

The author gratefully acknowledges fruitful discussions and helpful remarks from G. Pozzi, A. Tonomura, M. De Graef, and Y. Zhu.

[1] A. Tonomura, H. Kasai, O. Kamimura, T. Matsuda, K. Harada, Y. Nakayama, J. Shimonama, K. Kishio, T. Hanaguri, K. Kitazawa, M. Sanase, and S. Okayasu, Nature (London) **412**, 620 (2001).
[2] T. Matsuda, O. Kamimura, H. Kasai, K. Harada, T. Yoshida, T. Akashi, A. Tonomura, Y. Nakayama, J. Shimoyama, K. Kishio, T. Hanaguri, and K. Kitazawa, Science **294**, 2136 (2001).
[3] A. Tonomura, H. Kasai, O. Kamimura, T. Matsuda, K. Harada, T. Yoshida, T. Akashi, J. Shimoyama, K. Kishio, T. Hanaguri, K. Kitazawa, T. Matsui, S. Tajima, N. Koshizuka, P.L. Gammel, D. Bishop, M. Sasase, and S. Okayasu, Phys. Rev. Lett. **88**, 237001 (2002).
[4] A.E. Koshelev, Phys. Rev. Lett. **83**, 187 (1999).
[5] J.R. Clem and M.W. Coffey, Phys. Rev. B **42**, 6209 (1990).
[6] V.G. Kogan, V.V. Dobrovitski, J.R. Clem, Y. Mawatari, and R.G. Mints, Phys. Rev. B **63**, 144501 (2001).
[7] M. Beleggia and G. Pozzi, Ultramicroscopy **84**, 171 (2000).
[8] M. Beleggia and G. Pozzi, Phys. Rev. B **63**, 054507 (2001).
[9] M. Beleggia, G. Pozzi, J. Masuko, N. Osakabe, K. Harada, T. Yoshida, O. Kamimura, H. Kasai, T. Matsuda, and A. Tonomura, Phys. Rev. B **66**, 174518 (2002).
[10] A. Fukuhara, K. Shinagawa, A. Tonomura, and H. Fujiwara, Phys. Rev. B **27**, 1839 (1983).
[11] G. Pozzi, Adv. Imaging Electron Phys. **93**, 173 (1995).
[12] C. Capiluppi, G. Pozzi, and U. Valdrè, Philos. Mag. **26**, 865 (1973).
[13] J. Pearl, Appl. Phys. Lett. **5**, 65 (1964).
[14] T. Kawasaki, T. Yoshida, T. Matsuda, N. Osakabe, A. Tonomura, I. Matsui, and K. Kitazawa, Appl. Phys. Lett. **76**, 1342 (2000).
[15] A. Tonomura, *Electron Holography* (Springer, Berlin, 1993).
[16] K. Yamamoto, I. Kawajiri, T. Tanji, M. Hibino, and T. Hirayama, J. Electron Microsc. **49**, 31 (2000).
[17] O. Kamimura, H. Kasai, T. Akashi, T. Matsuda, K. Harada, J. Masuko, T. Yoshida, N. Osakabe, A. Tonomura, M. Beleggia, G. Pozzi, Y. Nakayama, J. Shimoyama, K. Kishio, T. Hanaguri, K. Kitazawa, M. Sasase, and S. Okayasu, J. Phys. Soc. Jpn. **71**, 1840 (2002).